Research Article

Rajneesh Kumar and Richa Vohra*

Response of thermoelastic microbeam with double porosity structure due to pulsed laser heating

https://doi.org/10.2478/mme-2019-0011
Received Jan 25, 2018; revised Sep 10, 2018; accepted Nov 20, 2018

Abstract: The present investigation is concerned with vibration phenomenon of a homogeneous, isotropic thermoelastic microbeam with double porosity (TDP) structure induced by pulsed laser heating, in the context of Lord–Shulman theory of thermoelasticity with one relaxation time. Laplace transform technique has been applied to obtain the expressions for lateral deflection, axial stress, axial displacement, volume fraction field, and temperature distribution. The resulting quantities are recovered in the physical domain by a numerical inversion technique. Variations of axial displacement, axial stress, lateral deflection, volume fraction field, and temperature distribution with axial distance are depicted graphically to show the effect of porosity and laser intensity parameter. Some particular cases are also deduced.

Keywords: double porosity, thermoelasticity, Lord–Shulman theory, laser pulse, microbeam

1 Introduction

The demand for engineering structures is continuously increasing. Aerospace vehicles, bridges, and automobiles are examples of these structures. Many aspects have to be taken into consideration in the design of these structures to improve their performance and extend their life. Micro- and nano-mechanical resonators have attracted considerable attention because of their many important technological applications. In the recent years, the laser pulse technology has been widely used in the material processing and nondestructive testing. Ultra-short lasers are those with pulse duration ranging from nanoseconds to femtoseconds in general. The irradiation of the surface of a solid by pulsed laser light generates wave motion in the solid material. During pulsed laser heating, thermoelastic waves are generated because of thermal expansion in the region near the surface that propagates into the target (microbeam).

Biot [1] proposed a model for porous media with single porosity. Later on, Barenblatt *et al.* [2] introduced a model for porous media with double porosity structure. Aifantis [3–5] used the mixture theory and studied the mechanics of diffusion in solids. Wilson and Aifantis [6] presented the theory of consolidation with the double porosity. Khalili [7] investigated the significance of the microscopic coupling effects on the response of double porosity media. Svanadze [8] studied the plane waves and boundary value problems in the theory of elasticity for solids with double porosity. Scarpetta and Svanadze [9] proved the uniqueness theorems in the quasi-static theory of thermoelasticity for solids with double porosity.

Cowin and Nunziato [10] developed a theory of linear elastic materials with voids for the mathematical study of the mechanical behavior of porous solids. In this theory, the skeletal materials are elastic and interstices are void of material; hence, an additional degree of freedom, the volume fraction of void, is added. Iesan and Quintanilla [11] derived a theory of thermoelastic solids with double porosity structure by using the theory developed by Cowin and Nunziato [10]. Darcy's law is not used in developing this theory. So far not much work has been done on the theory of thermoelasticity with double porosity based on the model proposed by Iesan and Quintanilla [11]. Recently, investigations on the theory of thermoelasticity with double porosity [11], which has a significant application in continuum mechanics, have been started. Kumar *et al.* [12] applied the state space approach to a boundary value problem for thermoelastic material with double porosity.

The thermoelastic waves induced by the laser pulse heating are investigated by various authors. Manolis and Beskos [13] examined the thermally induced vibration

***Corresponding Author: Richa Vohra:** Department of Mathematics & Statistics, Himachal Pradesh University, Shimla, Himachal Pradesh, India; Email: richavhr88@gmail.com
Rajneesh Kumar: Department of Mathematics, Kurukshetra University, Kurukshetra, Haryana, India

of structures consisting of beams exposed to rapid surface heating. Al-Huniti *et al.* [14] investigated the thermally induced displacements and stresses of a rod using the Laplace transformation technique. A problem of transverse vibrations of a beam induced by a mobile heat source is investigated by Kidawa [15]. Fang *et al.* [16] analyzed the frequency spectrum of laser-induced vibration of microbeams. Soh *et al.* [17] studied the vibration of micro/nanoscale beam resonators induced by ultra-short-pulsed laser by considering the thermoelastic coupling term. Sun *et al.* [18] investigated the vibration behavior of microbeam during pulsed laser heating. Othman *et al.* [19] studied the effect of initial stress on thermoelastic rotating medium with voids because of laser pulse heating with energy dissipation. Kumar [20] studied the response of thermoelastic beam because of thermal source in modified couple stress theory. Kaghazian *et al.* [21] investigated the free vibration analysis of a piezoelectric nanobeam using nonlocal elasticity theory. Zenkour [22] studied the thermoelastic response of a microbeam embedded in visco-Pasternak's medium based on GN-III model.

In the present article, response of a thermoelastic microbeam with double porosity (TDP) structure induced by laser pulse heating in the context of the Lord–Shulman theory of thermoelasticity is studied. Laplace transform has been applied to find the expressions for lateral deflection, axial stress, axial displacement, volume fraction field, and temperature distribution. The resulting quantities are obtained in the physical domain by using a numerical inversion technique. Variations of axial displacement, axial stress, lateral deflection, volume fraction field, and temperature distribution with axial distance are depicted graphically to show the effect of porosity and laser intensity parameter. Some special cases have also been deduced.

2 Basic equations

Following Iesan and Quintanilla [11] and Lord and Shulman [23], the field equations and constitutive relation for homogeneous, isotropic thermoelastic material with double porosity structure in the absence of body forces and extrinsic equilibrated body forces can be written as follows:

Equations of motion:

$$\mu\nabla^2 u_i + (\lambda+\mu)\, u_{j,ji} + b\varphi_{,i} + d\psi_{,i} - \beta T_{,i} = \rho\ddot{u}_i, \qquad (1)$$

Equilibrated stress equations of motion:

$$\alpha\nabla^2\varphi + b_1\nabla^2\psi - bu_{r,r} - \alpha_1\varphi - \alpha_3\psi + \gamma_1 T = \kappa_1\ddot{\varphi}, \qquad (2)$$

$$b_1\nabla^2\varphi + \gamma\nabla^2\psi - du_{r,r} - \alpha_3\varphi - \alpha_2\psi + \gamma_2 T = \kappa_2\ddot{\psi}, \qquad (3)$$

Equation of heat conduction:

$$\left(1+\tau_0\frac{\partial}{\partial t}\right)\left(\beta T_0\dot{u}_{j,j} + \gamma_1 T_0\dot{\varphi} + \gamma_2 T_0\dot{\psi} + \rho C^*\dot{T} - Q\right) = K^*\nabla^2 T, \qquad (4)$$

Constitutive relation:

$$t_{ij} = \lambda e_{rr}\delta_{ij} + 2\mu e_{ij} + b\varphi\delta_{ij} + d\psi\delta_{ij} - \beta T\delta_{ij}, \qquad (5)$$

where λ and μ are Lame's constants; ρ; is the mass density; $\beta = (3\lambda+2\mu)\,\alpha_t$; α_t is the linear thermal expansion; C^* is the specific heat at constant strain; u_i is the displacement components; t_{ij} is the stress tensor; κ_1 and κ_2 are coefficients of equilibrated inertia; φ is the volume fraction field corresponding to pores; ψ is the volume fraction field corresponding to fissures; K^* is the coefficient of thermal conductivity; τ_0 is the thermal relaxation time; Q is the heat source; κ_1 and κ_2 are coefficients of equilibrated inertia; $b, d, b_1, \gamma, \gamma_1, \gamma_2$ are constitutive coefficients; δ_{ij} is Kronecker's delta; T is the temperature change measured from the absolute temperature T_0 ($T_0 \neq 0$); and a superposed dot represents differentiation with respect to time variable t.

3 Formulation of the problem

Consider a homogeneous, isotropic, TDP structure having the dimensions length = $L\,(0 \le x \le L)$, width = $a\left(-\frac{a}{2} \le y \le \frac{a}{2}\right)$, and thickness = $h\left(-\frac{h}{2} \le z \le \frac{h}{2}\right)$ in a Cartesian coordinate system $Oxyz$ as shown in Figure 1.

The microbeam undergoes bending vibrations of small amplitude about the x-axis such that the deflection is consistent with the linear Euler–Bernoulli theory. Therefore, the displacements can be written as

$$u_1 = u = -z\frac{\partial w}{\partial x}, \quad u_2 = 0, \quad u_3 = w(x,t), \qquad (6)$$

where w is the lateral deflection and u is the axial displacement.

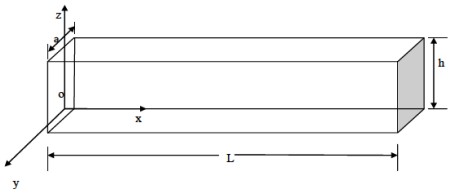

Figure 1: Geometry of the beam

The equation of motion for free flexural vibrations of the beam is given by

$$\frac{\partial^2 M}{\partial x^2} + \rho A\left(\frac{\partial^2 w}{\partial t^2}\right) = 0, \tag{7}$$

where $A = ah$ is the cross-sectional area and M is the flexural moment of cross section of microbeam. The flexural moment of the cross section of the beam is given by

$$M(x,t) = -a\int_{-h/2}^{h/2} t_x z dz = (\lambda + 2\mu) I\frac{\partial^2 w}{\partial x^2} - M_\varphi - M_\psi + M_T, \tag{8}$$

where $I = ah^3/12$ is the moment of inertia of the cross section; M_φ, M_ψ are the volume fraction field moments, and M_T is the thermal moment of the beam and are given by

$$M_\varphi = b\int_{-h/2}^{h/2} a\varphi z dz, \quad M_\psi = d\int_{-h/2}^{h/2} a\psi z dz, \quad M_T = \beta\int_{-h/2}^{h/2} aTz dz. \tag{9}$$

Substituting Eq. (8) in Eq. (7), we get the following equation of motion of the microbeam:

$$(\lambda + 2\mu) I\frac{\partial^4 w}{\partial x^4} + \rho A\left(\frac{\partial^2 w}{\partial t^2}\right) - \frac{\partial^2 M_\varphi}{\partial x^2} - \frac{\partial^2 M_\psi}{\partial x^2} + \frac{\partial^2 M_T}{\partial x^2} = 0. \tag{10}$$

Equations (2)–(4) with the aid of Eq. (6) can be written as follows:

$$\alpha\left(\frac{\partial^2 \varphi}{\partial x^2} + \frac{\partial^2 \varphi}{\partial z^2}\right) + b_1\left(\frac{\partial^2 \psi}{\partial x^2} + \frac{\partial^2 \psi}{\partial z^2}\right) + bz\frac{\partial^2 w}{\partial x^2} - \alpha_1\varphi - \alpha_3\psi + \gamma_1 T = \kappa_1\frac{\partial^2 \varphi}{\partial t^2} \tag{11}$$

$$b_1\left(\frac{\partial^2 \varphi}{\partial x^2} + \frac{\partial^2 \varphi}{\partial z^2}\right) + \gamma\left(\frac{\partial^2 \psi}{\partial x^2} + \frac{\partial^2 \psi}{\partial z^2}\right) + dz\frac{\partial^2 w}{\partial x^2} - \alpha_3\varphi - \alpha_2\psi + \gamma_2 T = \kappa_2\frac{\partial^2 \psi}{\partial t^2} \tag{12}$$

$$K^\star\left(\frac{\partial^2 T}{\partial x^2} + \frac{\partial^2 T}{\partial z^2}\right) = \left(1 + \tau_0\frac{\partial}{\partial t}\right)\left[-\beta T_0 z\frac{\partial}{\partial t}\left(\frac{\partial^2 w}{\partial x^2}\right) + \gamma_1 T_0\dot{\varphi} + \gamma_2 T_0\dot{\psi} + \rho C^\star\dot{T} - Q\right]. \tag{13}$$

The initial temperature distribution $T(x,z,0) = T_0$. For $t = 0$, the upper surface, $z = h/2$, of the beam is heated uniformly by a laser pulse with non-Gaussian form temporal profile, which can be written as

$$I(t) = \frac{I_0}{t_p^2} t e^{-\frac{t}{t_p}},$$

where t_p is a characteristics time of the laser pulse and I_0 is the laser intensity, which is defined as the total energy carried by a laser pulse per unit cross section of the laser beam. In accordance with Sun *et al.* [18], the thermal conduction in the beam can be modeled as a one-dimensional problem with an energy source $Q(z,t)$, that is,

$$Q(z,t) = \frac{R_a}{\delta_0} e^{\left(\frac{z-h/2}{\delta_0}\right)} I(t) = \frac{I_0 R_a t}{\delta_0 t_p^2} e^{\left(\frac{z-h/2}{\delta_0} - \frac{t}{t_p}\right)}, \tag{14}$$

where δ_0 is the absorptive depth of heating energy and R_a is the absorptivity of the irradiated surface.

4 Solution of the problem

For the present microbeam, we assume that there is no flow of heat and volume fraction fields across the surfaces ($z = \pm h/2$) so that $\partial T/\partial z = \partial\varphi/\partial z = \partial\psi/\partial z = 0$ at $z = \pm h/2$. For a very thin beam, assume that volume fraction fields and temperature increment in terms of $\sin(\pi z/h)$ function along the thickness direction. Therefore,

$$\varphi(x,z,t) = \Phi(x,t)\sin(\pi z/h), \quad \psi(x,z,t) = \Psi(x,t)\sin(\pi z/h), \quad T(x,z,t) = \Theta(x,t)\sin(\pi z/h). \tag{15}$$

Substituting Eq. (15) in Eq. (10) yields

$$(\lambda + 2\mu) I\frac{\partial^4 w}{\partial x^4} + \rho ah\left(\frac{\partial^2 w}{\partial t^2}\right) - \frac{2abh^2}{\pi^2}\frac{\partial^2 \Phi}{\partial x^2} - \frac{2adh^2}{\pi^2}\frac{\partial^2 \Psi}{\partial x^2} + \frac{2a\beta h^2}{\pi^2}\frac{\partial^2 \Theta}{\partial x^2} = 0. \tag{16}$$

Multiplying Eqs. (11)–(13) by z and integrating them with respect to z from $-h/2$ to $h/2$, we get

$$\alpha\left(\frac{\partial^2 \Phi}{\partial x^2} - \frac{\pi^2\Phi}{h^2}\right) + b_1\left(\frac{\partial^2 \Psi}{\partial x^2} - \frac{\pi^2\Psi}{h^2}\right) + \frac{b\pi^2 h}{24}\frac{\partial^2 w}{\partial x^2} - \alpha_1\Phi - \alpha_3\Psi + \gamma_1\Theta = \kappa_1\frac{\partial^2 \Phi}{\partial t^2} \tag{17}$$

$$b_1\left(\frac{\partial^2\Phi}{\partial x^2}-\frac{\pi^2\Phi}{h^2}\right)+\gamma\left(\frac{\partial^2\Psi}{\partial x^2}-\frac{\pi^2\Psi}{h^2}\right)+\frac{d\pi^2h}{24}\frac{\partial^2 w}{\partial x^2} \quad (18)$$
$$-\alpha_3\Phi-\alpha_2\Psi+\gamma_2\Theta=\kappa_2\frac{\partial^2\Psi}{\partial t^2}$$

$$K^\star\left(\frac{\partial^2\Theta}{\partial x^2}-\frac{\pi^2\Theta}{h^2}\right)=\left(1+\tau_0\frac{\partial}{\partial t}\right) \quad (19)$$
$$\left[-\frac{\beta T_0\pi^2h}{24}\frac{\partial}{\partial t}\left(\frac{\partial^2 w}{\partial x^2}\right)+\gamma_1T_0\frac{\partial\Phi}{\partial t}\right.$$
$$\left.+\gamma_2T_0\frac{\partial\Psi}{\partial t}+\rho C^\star\frac{\partial\Theta}{\partial t}-Q_0te^{-t/t_p}\right],$$

where

$$Q_0=\frac{R_aI_0h}{2t_p^2}\left[\left(1+\frac{2\delta_0}{h}\right)e^{-h/\delta_0}+\left(1-\frac{2\delta_0}{h}\right)\right].$$

Introducing nondimensional variables as

$$x'=\frac{1}{L}x,\quad u'=\frac{1}{L}u,\quad w'=\frac{1}{L}w,\quad t_x'=\frac{t_x}{E}, \quad (20)$$
$$\Phi'=\frac{L}{\alpha}\Phi,\quad \Theta'=\frac{\beta}{E}\Theta,\quad t'=\frac{c_1}{L}t,$$
$$\tau_0'=\frac{c_1}{L}\tau_0,\quad \Psi'=\frac{L}{\alpha}\Psi,$$

where $c_1^2=\frac{\lambda+2\mu}{\rho}$ and $E=\frac{\mu(3\lambda+2\mu)}{\lambda+\mu}$ is Young's modulus.

Substituting Eqs. (20) in Eqs. (16)–(19), we obtain (suppressing primes for convenience)

$$\frac{\partial^4 w}{\partial x^4}+a_1\left(\frac{\partial^2 w}{\partial t^2}\right)-a_2\frac{\partial^2\Phi}{\partial x^2}-a_3\frac{\partial^2\Psi}{\partial x^2}+a_4\frac{\partial^2\Theta}{\partial x^2}=0 \quad (21)$$

$$a_5\frac{\partial^2\Phi}{\partial x^2}-a_6\Phi+a_7\frac{\partial^2\Psi}{\partial x^2}-a_8\Psi+a_9\frac{\partial^2 w}{\partial x^2}-a_{10}\Phi \quad (22)$$
$$-a_{11}\Psi+a_{12}\Theta-\frac{\partial^2\Phi}{\partial t^2}=0$$

$$a_{13}\frac{\partial^2\Phi}{\partial x^2}-a_{14}\Phi+a_{15}\frac{\partial^2\Psi}{\partial x^2}-a_{16}\Psi+a_{17}\frac{\partial^2 w}{\partial x^2} \quad (23)$$
$$-a_{18}\Phi-a_{19}\Psi+a_{20}\Theta-\frac{\partial^2\Psi}{\partial t^2}=0$$

$$\frac{\partial^2\Theta}{\partial x^2}-a_{21}\Theta=\left(1+\tau_0\frac{\partial}{\partial t}\right) \quad (24)$$
$$\left[a_{22}\frac{\partial}{\partial t}\left(\frac{\partial^2 w}{\partial x^2}\right)+a_{23}\frac{\partial\Phi}{\partial t}+a_{24}\frac{\partial\Psi}{\partial t}+a_{25}\frac{\partial\Theta}{\partial t}-Q_1te^{-t/t_p}\right],$$

where

$$a_1=\frac{\rho ahc_1^2L^2}{I(\lambda+2\mu)},\quad a_2=\frac{2abah^2}{I\pi^2(\lambda+2\mu)},\quad a_3=\frac{2adah^2}{I\pi^2(\lambda+2\mu)},$$
$$a_4=\frac{2ah^2EL}{I\pi^2(\lambda+2\mu)},\quad a_5=\frac{\alpha}{k_1c_1^2},\quad a_6=\frac{\alpha\pi^2L^2}{k_1c_1^2h^2},$$
$$a_7=\frac{b_1}{k_1{c_1}^2},\quad a_8=\frac{b_1\pi^2L^2}{k_1c_1^2h^2},\quad a_9=\frac{bh\pi^2L^2}{24\alpha k_1c_1^2},$$
$$a_{10}=\frac{\alpha_1L^2}{k_1c_1^2},\quad a_{11}=\frac{\alpha_3L^2}{k_1c_1^2},\quad a_{12}=\frac{\gamma_1EL^3}{\alpha\beta k_1c_1^2},$$
$$a_{13}=\frac{b_1}{k_2{c_1}^2},\quad a_{14}=\frac{b_1\pi^2L^2}{k_2c_1^2h^2},\quad a_{15}=\frac{\gamma}{k_2{c_1}^2},$$
$$a_{16}=\frac{\gamma\pi^2L^2}{k_2c_1^2h^2},\quad a_{17}=\frac{dh\pi^2L^2}{24\alpha k_2c_1^2},\quad a_{18}=\frac{\alpha_3L^2}{k_2c_1^2},$$
$$a_{19}=\frac{\alpha_2L^2}{k_2c_1^2},\quad a_{20}=\frac{\gamma_2EL^3}{\alpha\beta k_2c_1^2},\quad a_{21}=\frac{\pi^2L^2}{h^2},$$
$$a_{22}=-\frac{T_0hc_1\pi^2\beta^2}{24EK^\star},\quad a_{23}=\frac{\alpha\beta T_0\gamma_1c_1}{EK^\star},$$
$$a_{24}=\frac{\alpha\beta T_0\gamma_2c_1}{EK^\star},\quad a_{25}=\frac{\rho C^\star c_1L}{K^\star},\ Q_1=\frac{Q_0\beta L^3}{K^\star Ec_1}e^{-L/c_1}.$$

5 Initial and boundary conditions

The initial conditions of the problem are assumed to be homogeneous and are written as

$$w(x,t)\big|_{t=0}=\left.\frac{\partial w(x,t)}{\partial t}\right|_{t=0}=0 \quad (25)$$
$$\Phi(x,t)\big|_{t=0}=\left.\frac{\partial\Phi(x,t)}{\partial t}\right|_{t=0}=0$$
$$\Psi(x,t)\big|_{t=0}=\left.\frac{\partial\Psi(x,t)}{\partial t}\right|_{t=0}=0$$
$$\Theta(x,t)\big|_{t=0}=\left.\frac{\partial\Theta(x,t)}{\partial t}\right|_{t=0}=0.$$

These initial conditions are supplemented by considering that the two ends of the microbeam are clamped and held at a constant temperature with no change in the volume fraction fields. Mathematically, it can be written as

$$w(x,t)\big|_{x=0,L}=\left.\frac{\partial w(x,t)}{\partial x}\right|_{x=0,L}=0, \quad (26)$$
$$\Phi(x,t)\big|_{x=0,L}=0,\quad \Psi(x,t)\big|_{x=0,L}=0,\quad \Theta(x,t)\big|_{x=0,L}=\Theta_0.$$

6 Solution in the Laplace transform domain

Applying the Laplace transform defined by

$$\bar f(s)=L[f(t)]=\int_0^\infty f(t)\,e^{-st}dt \quad (27)$$

in Eqs. (21)–(24) under the initial conditions (25) and after some simplifications, we obtain

$$\left(D^{10}+B_1D^8+B_2D^6+B_3D^4+B_4D^2+B_5\right)(\overline{w}, \quad (28)$$
$$\overline{\Phi},\overline{\Psi},\overline{\Theta})=(0,G_1,G_2,G_3).$$

Here $D^{\mathrm{m}}=\frac{\mathrm{d}^{\mathrm{m}}}{\mathrm{dx}^{\mathrm{m}}}$; the expressions for B_1, B_2, B_3, B_4, B_5, G_1, G_2, G_3 are given in Appendix 1.

The solution of Eq. (28) in the Laplace transform domain can be written as

$$\overline{w} = \sum_{i=1}^{5} \left(D_i e^{-\lambda_i x} + D_{i+5} e^{\lambda_i x} \right) \tag{29}$$

$$\overline{\Phi} = H_1 + \sum_{i=1}^{5} g_{1i} \left(D_i e^{-\lambda_i x} + D_{i+5} e^{\lambda_i x} \right) \tag{30}$$

$$\overline{\Psi} = H_2 + \sum_{i=1}^{5} g_{2i} \left(D_i e^{-\lambda_i x} + D_{i+5} e^{\lambda_i x} \right) \tag{31}$$

$$\overline{\Theta} = H_3 + \sum_{i=1}^{5} g_{3i} \left(D_i e^{-\lambda_i x} + D_{i+5} e^{\lambda_i x} \right). \tag{32}$$

The expressions for g_{1i}, g_{2i}, g_{3i} $(i = 1, 2, 3, 4, 5)$; H_1, H_2, H_3 are given in Appendix 2.

Here $\pm\lambda_i$, $i = 1, 2, 3, 4, 5$, are the roots of the characteristic equation

$$\lambda^{10} + B_1\lambda^8 + B_2\lambda^6 + B_3\lambda^4 + B_4\lambda^2 + B_5 = 0. \tag{33}$$

Therefore, the axial displacement in the Laplace transform using Eq. (29) can be written as

$$\overline{u} = -z\frac{d\overline{w}}{dx} = -z\sum_{i=1}^{5} \left(-\lambda_i D_i e^{-\lambda_i x} + \lambda_i D_{i+5} e^{\lambda_i x} \right). \tag{34}$$

The boundary conditions (26) in the Laplace transform domain take the following form:

$$\begin{aligned} &\overline{w}(x,s)\big|_{x=0.L} = \left.\frac{d\overline{w}(x,s)}{\partial x}\right|_{x=0,L} = 0, \\ &\overline{\Phi}(x,s)\big|_{x=0,L} = 0, \quad \overline{\Psi}(x,s)\big|_{x=0,L} = 0, \\ &\overline{\Theta}(x,s)\big|_{x=0,L} = \frac{\Theta_0}{s} = \overline{F}(s). \end{aligned} \tag{35}$$

In order to determine the unknown parameters, substituting (29)–(32) in the boundary conditions (35), we obtain a system of 10 linear equations in the following matrix form:

$$[A]\,[D] = [Y], \tag{36}$$

where

$$[A] = \begin{bmatrix} 1 & 1 & 1 & 1 & 1 \\ e^{-\lambda_1 L} & e^{-\lambda_2 L} & e^{-\lambda_3 L} & e^{-\lambda_4 L} & e^{-\lambda_5 L} \\ -\lambda_1 & -\lambda_2 & -\lambda_3 & -\lambda_4 & -\lambda_5 \\ -\lambda_1 e^{-\lambda_1 L} & -\lambda_2 e^{-\lambda_2 L} & -\lambda_3 e^{-\lambda_3 L} & -\lambda_4 e^{-\lambda_4 L} & -\lambda_5 e^{-\lambda_5 L} \\ g_{11} & g_{12} & g_{13} & g_{14} & g_{15} \\ g_{11} e^{-\lambda_1 L} & g_{12} e^{-\lambda_2 L} & g_{13} e^{-\lambda_3 L} & g_{14} e^{-\lambda_4 L} & g_{15} e^{-\lambda_5 L} \\ g_{21} & g_{22} & g_{23} & g_{24} & g_{25} \\ g_{21} e^{-\lambda_1 L} & g_{22} e^{-\lambda_2 L} & g_{23} e^{-\lambda_3 L} & g_{24} e^{-\lambda_4 L} & g_{25} e^{-\lambda_5 L} \\ g_{31} & g_{32} & g_{33} & g_{34} & g_{35} \\ g_{31} e^{-\lambda_1 L} & g_{32} e^{-\lambda_2 L} & g_{33} e^{-\lambda_3 L} & g_{34} e^{-\lambda_4 L} & g_{35} e^{-\lambda_5 L} \end{bmatrix}$$

$$\begin{bmatrix} \cdots & 1 & 1 & 1 & 1 & 1 \\ \cdots & e^{\lambda_1 L} & e^{\lambda_2 L} & e^{\lambda_3 L} & e^{\lambda_4 L} & e^{\lambda_5 L} \\ \cdots & \lambda_1 & \lambda_2 & \lambda_3 & \lambda_4 & \lambda_5 \\ \cdots & \lambda_1 e^{\lambda_1 L} & \lambda_2 e^{\lambda_2 L} & \lambda_3 e^{\lambda_3 L} & \lambda_4 e^{\lambda_4 L} & \lambda_5 e^{\lambda_5 L} \\ \cdots & g_{11} & g_{12} & g_{13} & g_{14} & g_{15} \\ \cdots & g_{11} e^{\lambda_1 L} & g_{12} e^{\lambda_2 L} & g_{13} e^{\lambda_3 L} & g_{14} e^{\lambda_4 L} & g_{15} e^{\lambda_5 L} \\ \cdots & g_{21} & g_{22} & g_{23} & g_{24} & g_{25} \\ \cdots & g_{21} e^{\lambda_1 L} & g_{22} e^{\lambda_2 L} & g_{23} e^{\lambda_3 L} & g_{24} e^{\lambda_4 L} & g_{25} e^{\lambda_5 L} \\ \cdots & g_{31} & g_{32} & g_{33} & g_{34} & g_{35} \\ \cdots & g_{31} e^{\lambda_1 L} & g_{32} e^{\lambda_2 L} & g_{33} e^{\lambda_3 L} & g_{34} e^{\lambda_4 L} & g_{35} e^{\lambda_5 L} \end{bmatrix}$$

$$[D] = \begin{bmatrix} D_1 & D_2 & D_3 & D_4 & D_5 & D_6 & D_7 & D_8 & D_9 & D_{10} \end{bmatrix}^{tr},$$

$$[Y] = \begin{bmatrix} 0 & 0 & 0 & 0 & -H_1 & -H_1 & -H_2 & -H_2 & H_4 & H_4 \end{bmatrix}^{tr},$$

$$H_4 = \overline{F}(s) - H_3,$$

tr is the transpose of the matrix.

By solving Eq. (36), we obtain the values of unknown parameters, D_i, $i = 1, 2, \ldots, 10$.

This completes the solution of the problem in the Laplace transform domain.

7 Particular cases

Case 1. If $\tau_0 = 0$ in Eq. (36), it yields the corresponding expressions for a TDP structure in the context of coupled theory (CT) of thermoelasticity.

Case 2. If $b_1 = \alpha_3 = \gamma = \alpha_2 = \gamma_2 = d \to 0$ in Eq. (36), we obtain the corresponding expressions for a thermoelastic microbeam with single porosity (TSP).

8 Inversion of the Laplace domain

To determine the lateral deflection, axial stress, axial displacement, volume fraction field, and temperature distribution in the physical domain, we adopt a numerical inversion method given by Honig and Hirdes [24].

In this method, the Laplace domain $\overline{f}(s)$ can be inverted to time domain $f(t)$ as follows:

$$f(t) = \frac{e^{\Omega t}}{t_1}\left[\frac{1}{2}\overline{f}(\Omega) + \mathrm{Re}\sum_{k=1}^{N}\overline{f}\left(\Omega + \frac{\iota k\pi}{t_1}\right)\exp\left(\frac{\iota k\pi t}{t_1}\right)\right],$$

$$0 < t_1 < 2t,$$

where Re is the real part and ι is the imaginary number unit. The value of N is chosen sufficiently large, and it represents the number of terms in the truncated Fourier series such that

$$f(t) = \exp(\Omega t)\mathrm{Re}\left[\bar{f}\left(\Omega + \frac{\iota N\pi}{t_1}\right)\exp\left(\frac{\iota N\pi t}{t_1}\right)\right] \leq \varepsilon_1,$$

where ε_1 is a prescribed small positive number. Also, the value of Ω should satisfy the relation $\Omega t \simeq 4.7$ for the faster convergence [25].

9 Numerical results and discussion

Numerical computations have been performed for copper-like material microbeam. The material parameters are taken as in Kumar *et al.* [12] $\lambda = 7.76 \times 10^{10}$ N m^{-2}, $C^\star = 3.831 \times 10^3$ m^2 s^{-2} K^{-1}, $\mu = 3.86 \times 10^{10}$ N m^{-2}, $K^\star = 3.86 \times 10^3$ N s^{-1} K^{-1}, $T_0 = 298$ K, $\rho = 8.954 \times 10^3$ kg m^{-3}, $\alpha_t = 1.78 \times 10^{-5}$ K^{-1}, $\alpha_2 = 2.4 \times 10^{10}$ N m^{-2}, $\alpha_3 = 2.5 \times 10^{10}$ N m^{-2}, $\gamma = 1.1 \times 10^{-5}$ N, $\alpha = 1.3 \times 10^{-5}$ N, $\gamma_2 = 0.219 \times 10^5$ N m^{-2}, $\kappa_1 = 0.1456 \times 10^{-12}$ N m^{-2} s^2, $b = 0.9 \times 10^{10}$ N m^{-2} $\alpha_1 = 2.3 \times 10^{10}$ N m^{-2}, $\kappa_2 = 0.1546 \times 10^{-12}$ N m^{-2} s^2, $\tau_0 = 0.01$ s.

The aspect ratio of the beam is fixed as $L/h = 10$, $a/h = 0.5$, and $z = h/6$. The laser pulse parameters are $t_p = 2$ ps, $I_0 = 1 \times 10^{11}$ J m^2, and $R_a = 0.5$, which are similar to that in Sun *et al.* [18]. The software MATLAB has been used to find the values of lateral deflection, axial stress, axial displacement, volume fraction field, and temperature distribution. The variations of these quantities with respect to axial distance have been given in Figures 2–11. In Figures 2–6, the graphical representation of the effect of porosity is given. In these figures, solid line corresponds to TDP and small dashes line corresponds to TSP. Also, the graphical representation of the effect of laser intensity parameter is depicted in Figures 7–11. In Figures 7–11, solid line, line with small dashes, and line with big dashes correspond to the values of laser intensity parameters $I_0 = 1 \times 10^{11}$, 2×10^{11}, and 3×10^{11}, respectively.

9.1 Effect of porosity

Figure 2 shows that for both TDP and TSP, the value of axial displacement, u, initially decreases for the region $0 < x < 1$ and increases afterwards in the remaining region with the increase in the value of x. Although the trend and behavior of variation of u is similar for both TDP and TSP for all the values of x but the magnitude values are more for TSP in comparison to TDP because of the effect of porosity. From Figure 3, it is noticed that for TDP, the values of lateral deflection w decreases for $0 < x < 1$, increases for $1 \leq x < 2$, and becomes almost stationary as $x \geq 2$, whereas in the case of TSP, it initially decreases for $0 < x < 1$ and then increases slowly and steadily as $x \geq 1$. The effect of porosity decreases the magnitude values of TSP compared to that of TDP. From Figure 4, it is clear that for TDP, the value of volume fraction field φ initially decreases sharply for the region $0 < x < 1$ and then start increasing as $x \geq 1$, whereas in the case of TSP, the value of φ initially increases for $0 < x < 1$ and then decreases slowly and steadily as $x \geq 1$. An opposite trend and behavior of variation is noticed for TDP and TSP. Also, the magnitude values of φ remain more for TSP as compared to TDP for

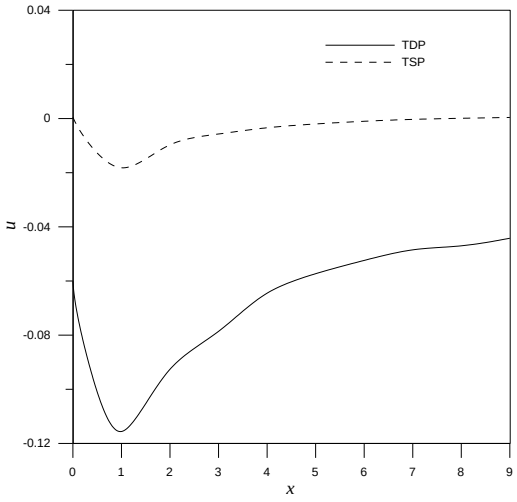

Figure 2: Variation of the axial displacement u with respect to the axial distance x

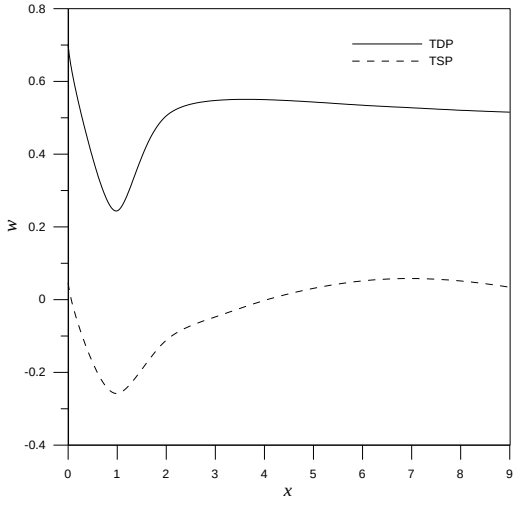

Figure 3: Variation of the lateral deflection w with respect to the axial distance x

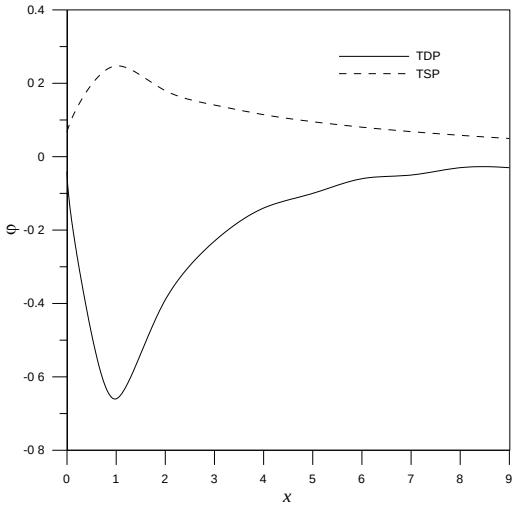

Figure 4: Variation of the volume fraction field φ with respect to the axial distance x

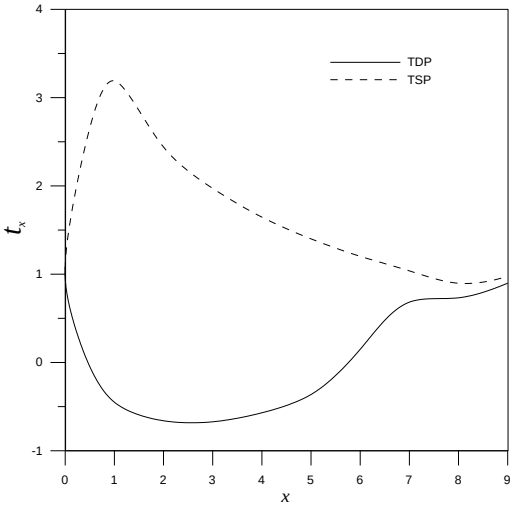

Figure 6: Variation of the axial stress t_x with respect to the axial distance x

all the values of x. Figure 5 shows that the value of temperature distribution, T, increases monotonically with the increase in the value of$x$. Although a similar trend of variation is noticed for both the materials but because of the effect of porosity, the magnitude values for TDP are higher in comparison to TSP. Figure 6 depicts that the value of axial stress, t_x, initially decreases for the region $0 < x < 3$ and increases afterwards in the remaining region in the case of TDP, whereas for TSP, it initially increases for $0 < x < 1$ and decreases as $x \geq 1$. The trend and behavior of variation is of opposite nature for TDP and TSP but the magnitude values are more for TSP in comparison to TDP because of the effect of porosity.

9.2 Effect of laser intensity parameter

From Figure 7, it is noticed that the value of axial displacement, u, initially decreases for the region $0 < x < 1$ and increases afterwards in the remaining region for all the values of laser intensity, I_0. It is found that the magnitude value of u decreases with the increase in the value of I_0. Figure 8 shows that the values of lateral deflection, w, decreases for $0 < x < 1$, increases for $1 < x < 3$, and becomes almost stationary as $x \geq 3$ for all the values of I_0. Also, the magnitude value of w decreases with the increase in the value of I_0. Figure 9 depicts that the value of volume fraction field, φ, initially decreases sharply for the region $0 < x < 1$ and then starts increasing monotonically as

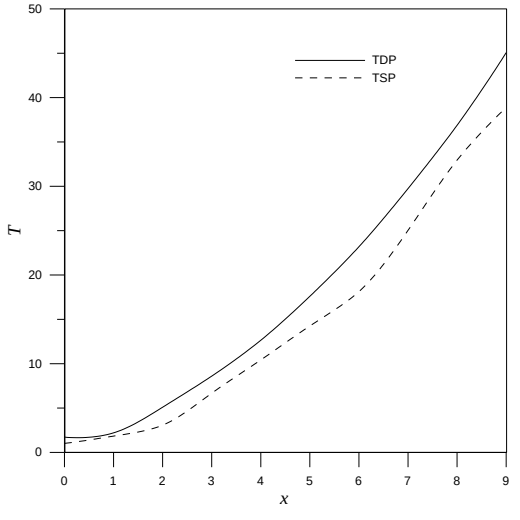

Figure 5: Variation of the temperature distribution T with respect to the axial distance x

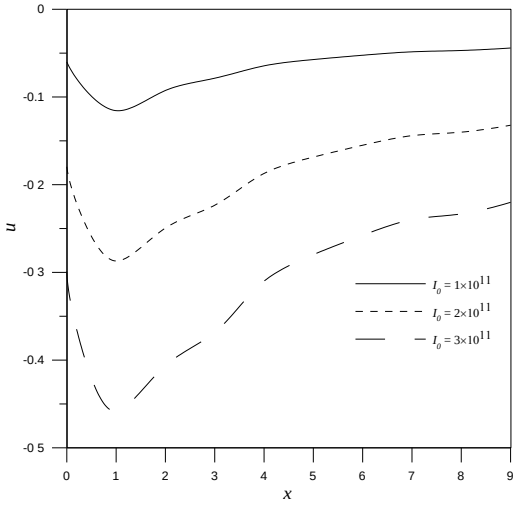

Figure 7: Variation of the axial displacement u with respect to the axial distance x

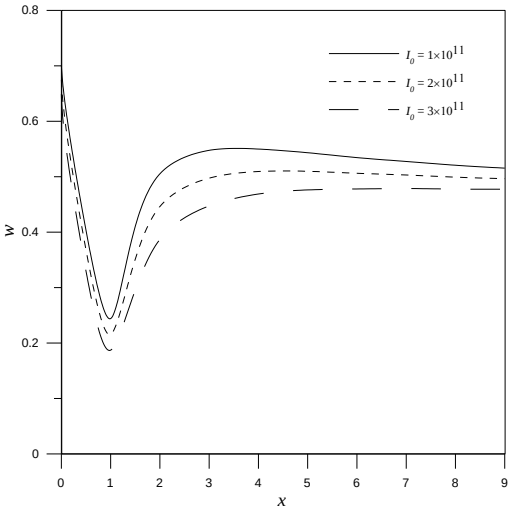

Figure 8: Variation of the lateral deflection w with respect to the axial distance x

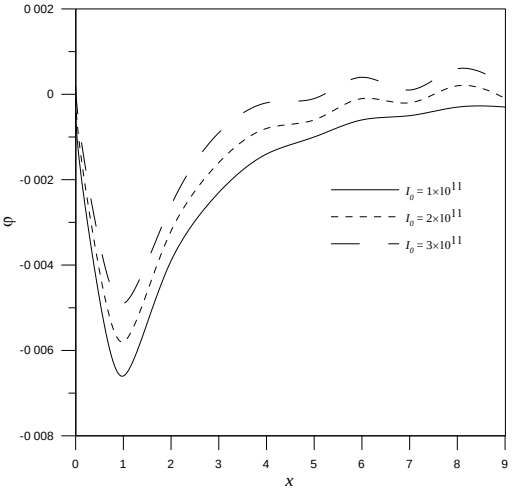

Figure 9: Variation of the volume fraction field φ with respect to the axial distance x

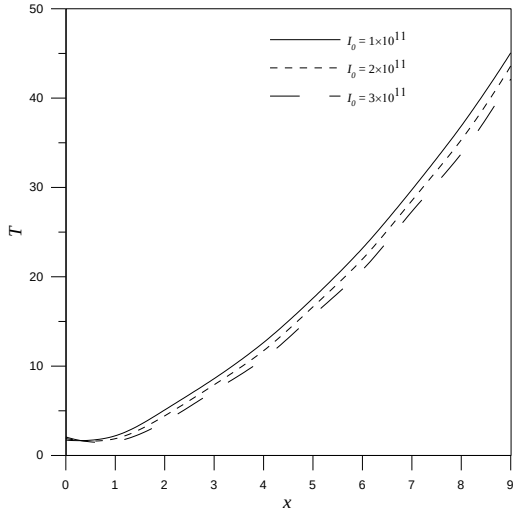

Figure 10: Variation of the temperature distribution T with respect to the axial distance x

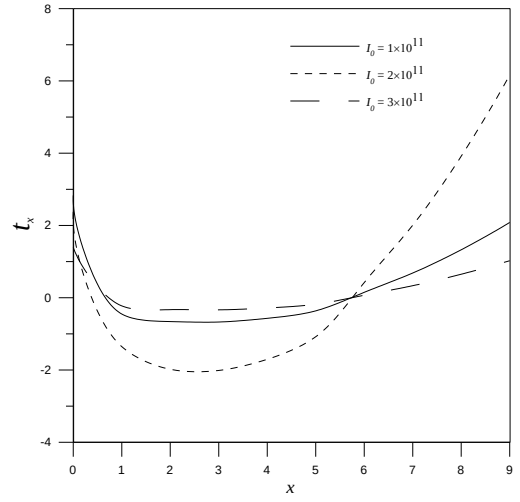

Figure 11: Variation of the axial stress t_x with respect to the axial distance x

$x \geq 1$. The magnitude value of φ increases with the increase in the value of I_0. From Figure 10, it is clear that the value of temperature distribution, T, increases monotonically with the increase in the value of x. It is also found that the magnitude values of T decreases with the increase in the value of laser intensity, I_0. From Figure 11, it is evident that the value of axial stress, t_x, initially decreases for $0 < x < 3$ and increases afterwards as $x \geq 3$. It is noticed that the magnitude value of t_x not necessarily increases or decreases with the variation in the value of laser intensity I_0.

10 Conclusions

In this work, vibration phenomenon of a homogeneous, isotropic TDP structure induced by pulsed laser heating in the context of the Lord–Shulman theory of thermoelasticity has been studied. The effects of porosity and laser intensity parameter on axial displacement, lateral deflection, volume fraction field, temperature distribution, and axial stress are graphically depicted. It is observed that the porosity has a significant effect on all the physical quantities. It has both increasing as well as decreasing effect on the resulting quantities. The magnitude values of lateral deflection and temperature distribution are more for TDP

in comparison to the values for TSP, whereas an opposite trend is noticed in the case of axial displacement, volume fraction field, and axial stress. Also, all the field quantities are observed to be very sensitive toward the laser intensity parameter, I_0. It is found that the magnitude values of axial displacement, lateral deflection, and temperature distribution decrease with the increases in the value of laser intensity parameter, whereas the trend gets reversed for the volume fraction field. Also, the magnitude values of axial stress not necessarily increase or decrease with the variation in the value of laser intensity parameter, I_0.

This type of study is useful because of its physical application in geophysics, rock mechanics, mechanical engineering, civil engineering, medical science, sensors, resonators, and so on.

References

[1] Biot, M.A.: General theory of three-dimensional consolidation, Journal of Applied Physics, 12, 155-164, 1941.

[2] Barenblatt, G.I ., Zheltov, I.P., Kochina, I.N.: Basic concept in the theory of seepage of homogeneous liquids in fissured rocks (strata), Journal of Applied Mathematics and Mechanics, 24, 1286-1303, 1960.

[3] Aifantis, E.C.: Introducing a multiporous medium, Developments in Mechanics, 8, 209-211, 1977.

[4] Aifantis, E.C.: On the response of fissured rock, Developments in Mechanics, 10, 249-253, 1979.

[5] Aifantis, E.C.: On the problem of diffusion in solids, Acta Mechanica, 37, 265-296, 1980.

[6] Wilson, R.K., Aifantis, E.C.: On the theory of consolidation with double porosity, International Journal of Engineering Science, 20(9), 1009-1035, 1984.

[7] Khalili, N.: Coupling effects in double porosity media with deformable matrix, Geophysics Research Letters, 30(22), 2153, DOI 10.1029/2003GL018544, 2003.

[8] Svanadze, M.: Plane waves and boundary value problems in the theory of elasticity for solids with double porosity, Acta Applicandae Mathematicae, 122, 461-470, 2012.

[9] Scarpetta, E., Svanadze, M.: Uniqueness theorems in the quasi-static theory of thermo elasticity for solids with double porosity, Journal of Elasticity, 120, 67–86, 2015.

[10] Cowin, S.C., Nunziato, J.W.: Linear elastic materials with voids, Journal of Elasticity, 13, 125-147, 1983.

[11] Iesan, D., Quintanilla, R.: On a theory of thermoelastic materials with a double porosity structure, Journal of Thermal Stresses, 37, 1017-1036, 2014.

[12] Kumar, R., Vohra, R., Gorla, G.: State space approach to boundary value problem for thermoelastic material with double porosity, Applied Mathematics and Computation, 271, 1038–1052, 2015.

[13] Manolis, G.D., Beskos, E.: Thermally induced vibrations of beam structures, Computer Methods in Applied Mechanics and Engineering, 21, 337–355, 1980.

[14] Al-Huniti, N.S., Al-Nimr, M.A. and Naij, M.: Dynamic response of a rod due to a moving heat source under the hyperbolic heat conduction model, Journal of Sound and Vibration, 242, 629–640, 2001.

[15] Kidawa, J.: Application of the Green functions to the problem of the thermally induced vibration of a beam, Journal of Sound and Vibration, 262, 865–876, 2003.

[16] Fang, D.N., Sun, Y.X., Soh, A.K.: Analysis of frequency spectrum of laser-induced vibration of microbeam resonators, Chinese Physics Letters, 23, 1554–1557, 2006.

[17] Soh, A.K., Sun, Y.X., Fang, D.N.: Vibration of microscale beam induced by laser pulse, Journal of Sound and Vibration, 311, 243-253, 2008.

[18] Sun, Y.X., Fang, D.N., Saka, M., Soh, A.K.: Laser induced vibrations of microbeams under different boundary conditions, International Journal of Solids and Structures, 45, 1993-2013, 2008.

[19] Othman, M.I.A., Zidan, M.E.M., Hilal, M.I.M.: The effect of initial stress on thermoelastic rotating medium with voids due to laser pulse heating with energy dissipation, Journal of Thermal Stresses, 38(8), 835-853, 2015.

[20] Kumar, R.: Response of thermoelastic beam due to thermal source in modified couple stress theory, Computational Methods in Science and Technology, 22(2), 95-101, 2016.

[21] Kaghazian, A., Hajnayeb, A., Foruzande, H.: Free vibration analysis of a piezoelectric nanobeam using nonlocal elasticity theory, Structural Engineering and Mechanics, 61(5), 617-624, 2017.

[22] Zenkour, A.M.: Thermoelastic response of a microbeam embedded in visco-Pasternak's medium based on GN-III model, Journal of Thermal Stresses, 40(2), 198–210, 2017.

[23] Lord, H., Shulman, Y.: A generalized dynamical theory of thermoelasticity, Journal of Mechanics and Physics of Solids, 15, 299-309, 1967.

[24] Honig, G., Hirdes, U.: A method for the numerical inversion of the Laplace transforms, Journal of Computational and Applied Mathematics, 10, 113-132, 1984.

[25] Tzou, D.: Macro-to-Micro Heat transfer, Taylor & Francis, Washington DC, 1996.

Appendix 1

$$a_{26} = s(1+\tau_0 s), \quad a_{27} = -s(1+\tau_0 s)a_{22},$$
$$a_{28} = -s(1+\tau_0 s)a_{23}, \quad a_{29} = -s(1+\tau_0 s)a_{24},$$
$$a_{30} = -\left\{a_{21} + s(1+\tau_0 s)a_{25}\right\},$$

$$n_1 = -\left(a_6 + a_{10} + s^2\right), \quad n_2 = -(a_8 + a_{11}),$$
$$n_3 = -(a_{18} + a_{14}), \quad n_4 = -\left(a_{16} + a_{19} + s^2\right),$$

$$r_1 = a_5 a_{15} - a_7 a_{13},$$

$$r_2 = a_5(a_{15}a_{30} + n_4) - a_{13}n_2 + n_1 a_{15} - a_7(a_{13}a_{30} + n_3),$$

$$r_3 = n_1(a_{15}a_{30} + n_4) + a_5(n_4 a_{30} - a_{20}a_{29})$$

$$- a_7(n_3a_{30} - a_{20}a_{28}) - n_2(a_{13}a_{30} + n_3) + a_{12}(a_{13}a_{29} - a_{15}a_{28}),$$

$$r_4 = n_1(n_4a_{30} - a_{20}a_{29}) + a_{12}(n_3a_{29} - n_4a_{28}) + n_2(a_{20}a_{28} - n_3a_{30}),$$

$$r_5 = a_9a_{15} - a_7a_{17},$$

$$r_6 = a_9(a_{15}a_{30} + n_4) - a_7(a_{17}a_{30} - a_{20}a_{27}) - n_2a_{17} - a_{12}a_{15}a_{27},$$

$$r_7 = a_9(n_4a_{30} - a_{20}a_{29}) + a_{12}(a_{17}a_{29} - n_4a_{27}) - n_2(a_{17}a_{30} - a_{20}a_{27}),$$

$$r_8 = a_9a_{13} - a_5a_{17},$$

$$r_9 = a_9(a_{13}a_{30} + n_3) - n_1a_{17} - a_5(a_{17}a_{30} - a_{20}a_{27}) - a_{12}a_{10}a_{27},$$

$$r_{10} = a_9(n_3a_{30} - a_{20}a_{28}) - n_1(a_{30}a_{17} - a_{27}a_{20}) + a_{12}\left(a_{17}a_{28} - n_3a_{27}\right),$$

$$r_{11} = a_{27}(a_5a_{12} + a_7a_{13}),$$

$$r_{12} = a_9(a_{13}a_{29} - a_{15}a_{28}) + a_5(n_4a_{27} - a_{17}a_{29}) + a_{27}(n_1a_{15} + g_3a_{13}) - a_7(a_{17}a_{28} - n_3a_{27}),$$

$$r_{13} = a_9(n_3a_{29} - n_4a_{28}) - n_1(a_{17}a_{29} - n_4a_{27}) - n_2(a_{17}a_{28} - n_3a_{27}),$$

$$B_1 = (r_2 + a_2r_5 - a_3r_8 - a_4r_{11})/r_1,$$

$$B_2 = \left(a_1r_1s^2 + a_2r_6 - a_3r_9 - a_4r_{12} + r_3\right)/r_1,$$

$$B_3 = \left(a_1r_3s^2 + a_2r_7 - a_3r_{10} - a_4r_{13} + r_4\right)/r_1,$$

$$B_4 = \left(a_1r_3s^2\right)/r_1, \quad B_5 = \left(a_1r_4s^2\right)/r_1,$$

$$G_1 = Q_1a_1s^2\left(g_2a_{20} - g_4a_{12}\right),$$

$$G_2 = Q_1a_1s^2\left(g_1a_{20} - g_3a_{12}\right),$$

$$G_3 = Q_1a_1s^2\left(g_1g_4 - g_2g_3\right)$$

Appendix 2

$$g_{1i} = -\left\{r_5\lambda_i^6 + r_6\lambda_i^4 + r_7\lambda_i^2\right\}/\left\{r_1\lambda_i^6 + r_2\lambda_i^4 + r_3\lambda_i^2 + r_4\right\},$$

$$g_{2i} = \left\{r_8\lambda_i^6 + r_9\lambda_i^4 + r_{10}\lambda_i^2\right\}/\left\{r_1\lambda_i^6 + r_2\lambda_i^4 + r_3\lambda_i^2 + r_4\right\},$$

$$g_{3i} = -\left\{r_{11}\lambda_i^6 + r_{12}\lambda_i^4 + r_{13}\lambda_i^2\right\}/\left\{r_1\lambda_i^6 + r_2\lambda_i^4 + r_3\lambda_i^2 + r_4\right\};$$
$$i = 1, 2, 3, \ldots, 5$$

$$H_j = G_jr_1/a_1r_4s^2; \quad j = 1, 2, 3.$$